Leveraging Sparsity to Enhance Selectivity in Radar Tunable Architectures

M. M. Omati, S. M. Karbasi, *Senior Member, IEEE,* A. Amini, *Senior Member, IEEE*

***Abstract*—In this paper, within the radar context, we explore the development of decision-making approaches capable of effectively rejecting mismatched signals within Gaussian interference with an unfamiliar covariance matrix. To achieve this, we employ the least absolute shrinkage and selection operator (LASSO) optimization as a sparse recovery framework, solved efficiently using the alternating direction method of multipliers (ADMM), to amplify the precision in estimating the target angle of arrival (AOA). The outcomes of this estimation procedure serve as the foundation for the detection frameworks, whether the one-step detector (OSD) or the two-step detector (TSD) approaches that rely on the generalized likelihood ratio test (GLRT) and adaptive matched filter (AMF). Importantly, these decision-making protocols provide a descent balance between detection performance (for matching signals) and rejecting undesired signals. During the analysis phase, we evaluate the effectiveness of our introduced detectors in comparison to the existing selective counterparts. The findings indicate that our proposed detectors surpass their counterparts in rejecting undesired signals, while sustaining a commendable level of detection performance for matching signals. Additionally, unlike most alternative methods, our proposed detectors demonstrate an acceptable level of execution time.**

Keywords: Alternating direction method of multipliers (ADMM), angle of arrival (AOA), one-step detector (OSD), two-step detector (TSD).

I. Introduction

In recent years, the radar field has witnessed a growing interest in developing adaptive detection systems to tackle mismatched signals [1–32]. In real-world scenarios, environmental and equipment factors can cause the reflected signal from a target to deviate from the main beam's expected direction. Such deviations significantly degrade detection performance and increase the likelihood of inaccurate estimates of the target's directional parameters. Mismatched signals often stem from a variety of non-idealities, including the presence of coherent jammers, resilient targets in sidelobes, imperfect modeling of the main lobe's steering vector, multipath propagation, and uncertainties in array calibration [7]. Traditional adaptive detection algorithms, particularly those relying on the assumption of perfect alignment between nominal and actual steering vectors [16–22], display varying degrees of sensitivity when confronted with such mismatched signals. They can be categorized based on their directivity, which is defined as the ability to detect or suppress mismatched signals [23]:

One category consists of robust decision approaches, designed to deliver excellent detection performance in the presence of off-grid conditions caused by angle and/or Doppler quantization. Such conditions can result in the actual steering vector misaligning with the nominal one. Subspace detectors, such as those proposed in [33–37], can be placed in this category.

Another category includes selective decision frameworks, which excel at rejecting signals whose characteristics differ from those of the target signal. By focusing on identifying and discarding mismatched signals, these frameworks effectively minimize false alarms, as demonstrated in [2, 4, 19, 38].

In practical scenarios, selective detectors are particularly useful for managing crowded environments or countering electronic countermeasures, such as coherent jammers [39]. Meanwhile, robust architectures are well-suited for covering wide angular regions with a limited number of filters (pointing directions) or detecting mismatched signals within the main beam. It is important to note that while enhanced selectivity is advantageous, it often comes at the cost of matched detection performance. Conversely, robust architectures maintain strong matched detection capabilities [20, 40–60]. In this context, the adaptive matched filter (AMF) [18] exemplifies a robust receiver. On the other hand, Kelly's detector is classified as a moderately selective receiver [61]. Additional examples of selective receivers include the adaptive coherence estimator (ACE) [9], also known as the adaptive normalized matched filter, as well as the adaptive beamformer orthogonal rejection test (ABORT) and whitened-ABORT (W-ABORT) detectors [51–53], and the Rao detector [20].

Therefore, the need for a decision scheme adaptable to different scenarios has led to the development of tunable detectors. These detectors can adjust their focus through well-defined design parameters, offering a balanced compromise between matched detection proficiency and the rejection of undesired signals. This establishes a notable paradigm in adaptive signal processing. Various design approaches, such as the combination of decision statistics of existing detectors and subspace detection techniques, are considered for the creation of these tunable architectures. Each approach presents distinct advantages in achieving the delicate balance between focus and detection accuracy. For example, the two-stage approach, which employs two decision schemes with contrasting focus behaviors in sequence, emerges as a powerful tool in the design of tunable architectures [7–14]. It offers a complex balance between directivity control and matched detection performance across various operational thresholds.

A. Contributions

In this paper, we present novel adaptive radar detection structures designed to enhance selectivity while maintaining

M. M. Omati, S. M. Karbasi (Corresponding author), and A. Amini are with the department of Electrical Engineering, Sharif University of Technology, Tehran, Iran (email: mohammad_omati@yahoo.com, m.karbasi@sharif.edu, aamini@sharif.edu)

robust detection capabilities in the presence of Gaussian interference with unknown covariance. In our paper, we combine the least absolute shrinkage and selection operator (LASSO) optimization [62] as a sparsity-promoting algorithm, efficiently solved using the alternating direction method of multipliers (ADMM), with statistical hypothesis testing techniques such as the generalized likelihood ratio test (GLRT) [19] and the adaptive matched filter (AMF) [18]. The motivation for utilizing sparsity arises from the intrinsic nature of radar environments and the complexities of target detection in challenging scenarios. In radar applications, the number of targets within a given range bin is usually much smaller than the total number of potential azimuth bins, making the problem inherently sparse. By leveraging this sparsity, we can achieve more precise and computationally efficient results. To further enhance the removal of undesired non-zero entries that reflect the presence of spurious targets, the procedure is complemented by the Bayesian information criterion (BIC) for model-order selection [63]. The output vector estimated using BIC enhances precision and efficiency in achieving sparsity in the recovery process while simultaneously reducing the computational workload.

The estimation outcomes derived after the BIC process form the foundation for the development of two radar detector classes. The first class integrates our sparse recovery algorithm with traditional statistical hypothesis testing radar detection schemes using a logical AND operation, introducing the two-step detector (TSD). The second class modifies the formulation of statistical methods, adopting a one-step detector (OSD) approach to enhance hypothesis testing. Both detector classes, rooted in the fusion of sparse reconstruction with statistical detection theory, result in highly selective and adaptive radar architectures. They exhibit superior performance in mismatched scenarios, demonstrating enhanced selectivity and maximum detection probability compared to conventional statistical algorithms. Additionally, they maintain appropriate execution times while preserving the potential for effective detection in matched scenarios.

Notaion: We follow the convention of using boldface letters for vectors (e.g., $\mathbf{a}$ in lowercase) and matrices (e.g., $\mathbf{A}$ in uppercase). Transposition and conjugate transposition operations are denoted by $(.)^T$ and $(.)^\dagger$, respectively. $\mathbf{I}$ and $\mathbf{0}$ represent the identity and all 0 matrices, respectively, with their dimensions inferred from the context. The set of $M \times N$ matrices with complex-valued entries is denoted as $\mathbb{C}^{M\times N}$. The Euclidean norm of vector $\mathbf{a}$ and the Frobenius norm of matrix $\mathbf{A}$ are given by $\|\mathbf{a}\|_2$ and $\|\mathbf{A}\|_F$, respectively.

II. METHODOLOGY

Imagine a search radar system that employs a uniform linear array with N spatial channels and directs its beam toward a specific azimuth direction. The system gathers data from multiple range cells and assesses whether the data obtained from a particular range bin contains a mainbeam target. If a target is detected, the angle of arrival (AOA) and range are estimated. Typically, in the conventional detection procedure, each range cell is checked individually, and it is presumed that the actual target AOA corresponds to the nominal steering angle (i.e., the steering vector for the boresight). In this scenario, we are dealing with the detection problem for a specific range bin. The data received from radar signals for this bin is gathered into a one-dimensional vector, denoted as $\mathbf{y} \in \mathbb{C}^{N\times 1}$. This problem can be framed using the hypothesis test described below:

$$\begin{aligned} &H_1 : \mathbf{y} = x\,\mathbf{a}(\theta_p) + \boldsymbol{\nu}, \\ &H_0 : \mathbf{y} = \boldsymbol{\nu}. \end{aligned} \tag{1}$$

The variable $x \in \mathbb{C}$ accounts for the transmitting antenna gain, the radar cross-section (RCS) of the target (which fluctuates slowly), and two-way path loss. The interference component, denoted by the complex Gaussian random vector $\boldsymbol{\nu}$, encapsulates the total effect of clutter and noise with an unknown positive-definite covariance matrix $\mathbf{R}$. The parameter θ_p represents the nominal AOA of the target, which coincides with the beam-pointing direction. The nominal spatial steering vector is represented by:

$$\mathbf{a}(\theta_p) = \left[1, \mathrm{e}^{\mathrm{j}2\pi(d/\lambda)\sin(\theta_p)}, ..., \mathrm{e}^{\mathrm{j}(N-1)2\pi(d/\lambda)\sin(\theta_p)}\right]^T,$$

where d is the inter-element spacing, and λ is the operating wavelength. When H_1 is declared, the range associated with $\mathbf{y}$ and θ_p are returned as target parameter estimates. However, due to various factors, the ideal condition of a perfect match between the received echoes and the nominal steering vector may not be met in practice. Hence, it would be more reasonable to pursue the following alternative instead of problem (1):

$$\begin{aligned} &H_1 : \mathbf{y} = x\mathbf{a}(\theta_t) + \boldsymbol{\nu}, \\ &H_0 : \mathbf{y} = \boldsymbol{\nu}, \end{aligned} \tag{2}$$

where the variable θ_t represents the actual AOA of the structured data received from an object within the monitored area. This angle may differ from the assumed pointing direction θ_p. This model is more realistic than the previous one, as it accounts for scenarios where the organized aspect of the gathered data may originate from non-target objects. For instance, a coherent jammer could emit a signal that enters through the sidelobes and injects false data into the radar processor.

One possible approach to handle the aforementioned situations is to sequentially test various azimuth positions of the mainbeam. In this scenario, a secondary dataset $\mathbf{y}_k \in \mathbb{C}^{N\times 1}$ $(k = 1, ..., K)$ is assumed to be available that does not contain any useful signal component, but has the same spectral properties as the interference in $\mathbf{y}$ (i.e., a homogeneous environment). Based on this assumption, some classic decision rules such as Kelly's GLRT [19] and AMF [18] can be utilized to ensure highly matched detection performances. To be specific, the decision schemes for Kelly's GLRT and AMF for an angular position θ can be expressed as

$$\Pi_{\mathrm{GLRT}} = \frac{\left|\mathbf{a}^\dagger(\theta)\hat{\mathbf{R}}^{-1}\mathbf{y}\right|^2}{\left(\mathbf{a}^\dagger(\theta)\hat{\mathbf{R}}^{-1}\mathbf{a}(\theta)\right)\left(K + \mathbf{y}^\dagger\hat{\mathbf{R}}^{-1}\mathbf{y}\right)} \underset{\mathrm{H}_0}{\overset{\mathrm{H}_1}{\gtrless}} \kappa_{\mathrm{GLRT}}, \tag{3}$$

$$\Pi_{\text{AMF}} = \frac{\left|\mathbf{a}^{\dagger}(\theta)\hat{\mathbf{R}}^{-1}\mathbf{y}\right|^2}{\mathbf{a}^{\dagger}(\theta)\hat{\mathbf{R}}^{-1}\mathbf{a}(\theta)} \underset{\text{H}_0}{\overset{\text{H}_1}{\gtrless}} \kappa_{\text{AMF}}. \tag{4}$$

The variable $\hat{\mathbf{R}} = \frac{1}{K}\sum_{k=1}^{K}\mathbf{y}_k\mathbf{y}_k^{\dagger}$ represents the sample covariance matrix obtained from the training data, while κ_{GLRT} and κ_{AMF} are thresholds established to achieve a specific probability of false alarm (P_{fa}).
Kelly's GLRT and the AMF techniques maintain the constant false alarm rate (CFAR) property with regards to the interference covariance matrix. While they exhibit exceptional performance for matched signals, their ability to discriminate azimuth and reject unmatched signals is limited. This means that a target originating from a direction other than the intended pointing direction may produce several detections.

To overcome this limitation, we develop four new algorithms in this manuscript with adjustable architectures that leverage sparse reconstruction techniques to improve selectivity. More specifically, we divide the angular region covering the mainbeam and relevant sidelobes of the antenna into M azimuth bins with equal spacing $\Delta\theta$. Each azimuth bin has a center angle θ_l, where l ranges from 1 to M. We represent the echoes received from a specific range cell using the following model [7]:

$$\mathbf{y} = \sum_{l=1}^{M} x_l\mathbf{a}(\theta_l) + \boldsymbol{\nu} = \mathbf{A}\mathbf{x} + \boldsymbol{\nu}, \tag{5}$$

where $\mathbf{A} = [\mathbf{a}(\theta_1), \ldots, \mathbf{a}(\theta_M)] \in \mathbb{C}^{N\times M}$ represents the dictionary matrix, and $\mathbf{x} = [x_1, \ldots, x_M]^T \in \mathbb{C}^{M\times 1}$ is the vector containing the responses corresponding to potential targets.

Emphasizing the importance of two specific points is crucial. Primarily, the vector $\mathbf{x}$ in equation (5) assumes a sparse configuration, wherein only a single entry corresponds to the AOA of the target, with all other entries assuming null values. Subsequently, $\Delta\theta$ emerges as a pivotal tuning parameter, governing both angular estimation resolution and the caliber of estimation. Increasing the value of N ($\Delta\theta$) combined with decreasing the coherence of the dictionary result in better estimates within the sparse recovery framework, as expounded in the ensuing discourse. Furthermore, under the aforementioned prerequisites, the inner-product between contiguous columns of $\mathbf{A}$ decreases, thereby mitigating the spread of target energy across successive azimuth bins. Nevertheless, augmented values of $\Delta\theta$ concomitantly reduce the angular resolution pertinent to AOA estimation. Hence, the determination of a suitable range for $\Delta\theta$ necessitates meticulous scrutiny to establish an optimal trade-off between the precision of the estimates and their reliability, while also considering the specific use case of the radar system and its operating requirements [7].

In the subsequent section, we describe the sparse recovery algorithm employed for the estimation of $\mathbf{x}$, presupposing the accessibility of data for the interference covariance matrix assessment, and adhering to the constraint $N < M$ to attain an overdetermined model.

III. Sparse recovery algorithm

In this section, we describe the specific sparse recovery algorithm used for estimating $\mathbf{x}$, which involves solving the LASSO optimization problem. The motivation for leveraging sparsity to estimate $\mathbf{x}$ stems from the inherent characteristics of radar scenes and the challenges associated with target detection in complex environments. In most radar applications, the number of targets in a given range bin is typically small compared to the number of potential azimuth bins, meaning that $\mathbf{x}$ is naturally sparse. By exploiting this sparsity, we can achieve more accurate and efficient estimation of $\mathbf{x}$. Sparsity enables the algorithm to focus on the most significant target responses while ignoring irrelevant or spurious signals, leading to improved selectivity and robustness. This is particularly important in crowded or complex environments where traditional methods may struggle to resolve closely spaced targets or accurately estimate their parameters.

To solve the LASSO optimization problem efficiently, we employ the alternating direction method of multipliers (ADMM) [64, 65], a widely used numerical technique designed to address convex optimization problems with convex constraints and objective functions. ADMM decomposes the original problem into smaller, efficiently solvable subproblems, combining the decomposability of the dual ascent method with the superior convergence properties of the method of multipliers. This makes ADMM a powerful and flexible approach for sparse recovery.

Based on the characteristics mentioned above, a sparsity-promoting probability density function is utilized to enforce a sparsity constraint on $\mathbf{x}$:

$$f(\mathbf{x}) = \frac{1}{C}\prod_{k=1}^{M}\exp\{-2\mu|x_k|\}, \tag{6}$$

where μ represents the Lagrange multiplier, and C is a normalizing constant that can be disregarded without affecting the outcome. Our sparse recovery approach is based on the maximum a posteriori (MAP) strategy. As a result, if $\mathbf{y}$ and $\mathbf{R}$ are given, the estimation of $\mathbf{x}$ can be expressed as:

$$\hat{\mathbf{x}} = \arg\max_{\mathbf{x}} f(\mathbf{y} \mid \mathbf{x}; \mathbf{R}) f(\mathbf{x}), \tag{7}$$

where

$$f(\mathbf{y} \mid \mathbf{x}; \mathbf{R}) = \frac{1}{\pi^M \det(\mathbf{R})}\exp\left\{-\left\|\mathbf{R}^{-\frac{1}{2}}(\mathbf{y} - \mathbf{A}\mathbf{x})\right\|_2^2\right\} \tag{8}$$

represents the conditional probability density function (pdf) of $\mathbf{y}$ given $\mathbf{x}$. With some simplifications, it is possible to show that (7) is equivalent to

$$\hat{\mathbf{x}} = \arg\min_{\mathbf{x}} \boldsymbol{\Gamma}(\mathbf{x}, \mathbf{R}), \tag{9}$$

$$\boldsymbol{\Gamma}(\mathbf{x}, \mathbf{R}) = \frac{1}{2}\left\|\mathbf{R}^{-\frac{1}{2}}(\mathbf{y} - \mathbf{A}\mathbf{x})\right\|_2^2 + \mu\|\mathbf{x}\|_1. \tag{10}$$

Prior to addressing the problem outlined above, our attention is drawn to the interference covariance matrix $\mathbf{R}$, which is generally unknown in practice. To overcome this, the radar system collects training samples near the test cell that accurately represent the interference affecting the cell under test. Subsequently, in the following steps, we estimate $\mathbf{R}$ using the sample covariance matrix (SCM) based on secondary data, namely $\hat{\mathbf{R}}$. As a result, after substituting $\mathbf{R}$ with the corresponding estimate and making adjustments to the two variables $\mathbf{z} = \hat{\mathbf{R}}^{-\frac{1}{2}}\mathbf{y}$ and $\mathbf{\Psi} = \hat{\mathbf{R}}^{-\frac{1}{2}}\mathbf{A}$, the problem (10) is transformed into:

$$\hat{\mathbf{x}} = \arg\min_{\mathbf{x}} \tfrac{1}{2} \left\|\mathbf{z} - \mathbf{\Psi}\mathbf{x}\right\|_2^2 + \mu\|\mathbf{x}\|_1. \tag{11}$$

To solve problem (11), we propose an algorithm based on the ADMM. By introducing the auxiliary variable $\mathbf{w}$, problem (11) is transformed into:

$$\begin{aligned}\hat{\mathbf{x}}, \hat{\mathbf{w}} = \arg\min_{\mathbf{x},\mathbf{w}} \tfrac{1}{2} \left\|\mathbf{z} - \mathbf{\Psi}\mathbf{x}\right\|_2^2 + \mu\|\mathbf{w}\|_1,\\ s.t. \qquad \mathbf{x} = \mathbf{w}.\end{aligned} \tag{12}$$

Based on ADMM, the associated augmented Lagrangian (AL) function is defined as:

$$\begin{aligned}\mathcal{L}_\rho^{\mathbf{\Psi}}(\mathbf{x},\mathbf{w},\mathbf{r}) = \tfrac{1}{2} \left\|\mathbf{z} - \mathbf{\Psi}\mathbf{x}\right\|_2^2 + \mu\|\mathbf{w}\|_1 \\ + \rho \operatorname{Re}\left\{\mathbf{r}^H(\mathbf{x}-\mathbf{w})\right\} + \tfrac{\rho}{2}\left\|\mathbf{x}-\mathbf{w}\right\|_2^2,\end{aligned} \tag{13}$$

where $\mathbf{r}$ represents the Lagrange multiplier, and ρ is the penalty parameter. The optimization process involves minimizing $\mathcal{L}_\rho^{\mathbf{\Psi}}(\mathbf{x},\mathbf{w},\mathbf{r})$ with respect to the primal variables $\mathbf{x}$ and $\mathbf{w}$, and updating $\mathbf{r}$ to maximize the dual objective. These steps result in a series of subproblems. Consequently, the scaled form of ADMM is expressed as:

$$\mathbf{x}^{(t+1)} = \arg\min_{\mathbf{x}} \tfrac{1}{2} \left\|\mathbf{z}-\mathbf{\Psi}\mathbf{x}\right\|_2^2 + \tfrac{\rho}{2}\left\|\mathbf{x}-\mathbf{w}^{(t)}+\mathbf{r}^{(t)}\right\|_2^2, \tag{14}$$

$$\mathbf{w}^{(t+1)} = \arg\min_{\mathbf{w}} \tfrac{\mu}{\rho}\|\mathbf{w}\|_1 + \tfrac{1}{2}\left\|\mathbf{x}^{(t+1)}-\mathbf{w}+\mathbf{r}^{(t)}\right\|_2^2, \tag{15}$$

$$\mathbf{r}^{(t+1)} = \mathbf{r}^{(t)} + \mathbf{x}^{(t+1)} - \mathbf{w}^{(t+1)}. \tag{16}$$

The quadratic functions in (14) can be minimized efficiently by utilizing the first derivative. For the ℓ_1-norm in (15), the solution is found using the soft-thresholding function $\mathcal{S}_\delta(\mathbf{v}) = \operatorname{sgn}(\mathbf{v}) \cdot \max(|\mathbf{v}| - \delta; 0)$. Consequently, the solutions for each of the optimization problems in (14)-(16) can be derived from the following equations:

$$\mathbf{x}^{(t+1)} = \left(\mathbf{I} + \tfrac{1}{\rho}\mathbf{\Psi}^H\mathbf{\Psi}\right)^{-1}\left(\tfrac{1}{\rho}\mathbf{\Psi}^H\mathbf{z} + (\mathbf{w}^{(t)} - \mathbf{r}^{(t)})\right), \tag{17}$$

$$\mathbf{w}^{(t+1)} = \mathcal{S}_{\frac{\mu}{\rho}}\left(\mathbf{x}^{(t+1)} + \mathbf{r}^{(t)}\right), \tag{18}$$

$$\mathbf{r}^{(t+1)} = \mathbf{r}^{(t)} + \mathbf{x}^{(t+1)} - \mathbf{w}^{(t+1)}. \tag{19}$$

Although (17) presents a closed-form solution, the computation of the inverse matrix is impractical for large sizes. So, we can further simplify (17) based on the matrix inversion lemma

$$\left(\mathbf{I} + \tfrac{1}{\rho}\mathbf{\Psi}^H\mathbf{\Psi}\right)^{-1} = \mathbf{I} - \tfrac{1}{\rho}\mathbf{\Psi}^H\left(I + \tfrac{1}{\rho}\mathbf{\Psi}\mathbf{\Psi}^H\right)^{-1}\mathbf{\Psi}. \tag{20}$$

IV. BIC-Based Model-Order Selection

Although the LASSO optimization solution $\tilde{\mathbf{x}}$, solved using ADMM, may include more nonzero entries than the actual number of targets, its sparsity can be refined using the Bayesian information criterion (BIC) [63]. To estimate the number of targets, a hypothesized model order h (the number of significant nonzero entries) is considered. For each h, the BIC is defined as

$$BIC(h) \;=\; 2\left\|\mathbf{z} - \mathbf{\Psi}\,\tilde{\mathbf{x}}(h)\right\|_2^2 \;+\; 3\,h\,\ln(2N),$$

where $\tilde{\mathbf{x}}(h)$ is obtained by retaining the h largest entries of $\tilde{\mathbf{x}}$ (in magnitude) and setting the rest to zero. The coefficient 3 reflects the number of real-valued parameters estimated per target. For instance, each target is characterized by a complex amplitude (two real parameters) and an additional parameter such as angle, resulting in three real parameters per target.

The value of h is constrained to lie within the range $\{1, \ldots, h_{\max}\}$, where $h_{\max}$ represents the maximum anticipated number of targets. The optimal model order $\hat{h}$ is determined by minimizing the BIC: $\hat{h} = \arg\min_h BIC(h)$. Using this $\hat{h}$, the refined estimate of $\tilde{\mathbf{x}}$ is obtained as $\hat{\mathbf{x}} = \tilde{\mathbf{x}}(\hat{h})$, where only the $\hat{h}$ largest entries are retained.

In this paper, we refer to the combination of BIC and ADMM as BADMM.

V. Sparse Amplitude Estimation for Improved Decision Schemes

We now delve into the intricate domain of decision strategy formulation, harnessing the sparse amplitude estimate. To elaborate, if the value of $\hat{x}_m$, which represents a part of x related to the expected steering angle, is larger than the threshold $|\hat{x}_m| > 0$, the system confidently concludes the situation as H_1. However, given the impact of estimation errors, the sparse amplitude estimate may lack precision, and certain non-zero elements might not accurately signify the positions of genuine targets. To tackle this challenge, two distinct architectural approaches are elucidated in the ensuing subsections.

A. Two-stage decision architectures

The so-called two-stage architecture refers to the detectors in which the two decision schemes are interwoven in a cascading manner [6, 7, 15]. Designated as the two-step detectors (TSD), this methodology involves a logical AND operation between the outcomes of sparse reconstruction technique and the established CFAR detectors, as explained below:

TSD-AMF:

$$\begin{cases} H_0 : |\hat{x}_m| = 0 \text{ or } \Pi_{\text{AMF},m} < \kappa_{\text{AMF}} \\ H_1 : |\hat{x}_m| > 0 \text{ and } \Pi_{\text{AMF},m} > \kappa_{\text{AMF}}, \end{cases}$$

TSD-GLRT:

$$\begin{cases} H_0 : |\hat{x}_m| = 0 \text{ or } \Pi_{\text{GLRT},m} < \kappa_{\text{GLRT}} \\ H_1 : |\hat{x}_m| > 0 \text{ and } \Pi_{\text{GLRT},m} > \kappa_{\text{GLRT}}, \end{cases}$$

Here, the integer m stands for the index corresponding to the nominal pointing direction. The decision statistics, $\Pi_{\text{AMF},m}$ and $\Pi_{\text{GLRT},m}$, associated with the AMF and Kelly's GLRT, respectively, are determined through the utilization of the nominal steering vector $\mathbf{a}(\theta_m)$. Simultaneously, the detection thresholds for the AMF and Kelly's GLRT are represented by κ_{AMF} and κ_{GLRT}, respectively.

It is crucial to emphasize that the effective P_{fa} for TSD-AMF and TSD-GLRT are expressed as:

$$\begin{aligned}P_{fa,\text{TSD-AMF}} &= P(|\hat{x}_m| > 0, \Pi_{\text{AMF},m} > \kappa_{\text{AMF}}|H_0)\\ &\leq P(\Pi_{\text{AMF},m} > \kappa_{\text{AMF}}|H_0),\\ P_{fa,\text{TSD-GLRT}} &= P(|\hat{x}_m| > 0, \Pi_{\text{GLRT},m} > \kappa_{\text{GLRT}}|H_0)\\ &\leq P(\Pi_{\text{GLRT},m} > \kappa_{\text{GLRT}}|H_0).\end{aligned}$$

Consequently, the TSD-AMF and TSD-GLRT are commonly categorized as bounded CFAR techniques, given that AMF and Kelly's GLRT serve as CFAR detectors.

B. Likelihood-based decision architectures

An alternative method for developing detectors that effectively regulates the false alarm rate involves making specific adjustments to the GLRT. In this approach, certain parameters are treated as unknown and are estimated using the maximum likelihood method, while other parameters are substituted with appropriate estimates. In this scenario, the sparse amplitude estimates obtained from the previously outlined estimation procedure can be leveraged.

To be more specific, consider the integer m indexing the nominal steering direction. In this context, the likelihood ratio test (LRT) is defined as

$$\Pi_{\text{LRT},m} = \frac{f(\mathbf{y}, \mathbf{y}_1, \ldots, \mathbf{y}_K; x_m, \mathbf{R}, H_1)}{f(\mathbf{y}, \mathbf{y}_1, \ldots, \mathbf{y}_K; \mathbf{R}, H_0)} \underset{\text{H}_0}{\overset{\text{H}_1}{\gtrless}} \kappa, \tag{21}$$

where
$$f(\mathbf{y}, \mathbf{y}_1, \ldots, \mathbf{y}_K; x_m, \mathbf{R}, H_1) = \left(\frac{\exp\left(-\text{Tr}(\mathbf{R}^{-1}\mathbf{T}_1)\right)}{\pi^N \det(\mathbf{R})}\right)^{(K+1)}$$
and
$$f(\mathbf{y}, \mathbf{y}_1, \ldots, \mathbf{y}_K; \mathbf{R}, H_0) = \left(\frac{\exp\left(-\text{Tr}(\mathbf{R}^{-1}\mathbf{T}_0)\right)}{\pi^N \det(\mathbf{R})}\right)^{(K+1)}$$
represent the joint pdfs of the vectors $\mathbf{y}, \mathbf{y}_1, \ldots, \mathbf{y}_K$ under H_1 and H_0, respectively, if

$$\mathbf{T}_1 = \frac{\left(\mathbf{y} - x_m\mathbf{a}(\theta_m)\right)\left(\mathbf{y} - x_m\mathbf{a}(\theta_m)\right)^\dagger + K\hat{\mathbf{R}}}{K+1}, \tag{22}$$

$$\mathbf{T}_0 = \frac{\mathbf{y}\mathbf{y}^\dagger + K\hat{\mathbf{R}}}{K+1}. \tag{23}$$

Equation (21) demonstrates that the LRT for determining the standard angular position relies on two key factors: the target amplitude x_m and the interference covariance matrix $\mathbf{R}$. By substituting x_m with the estimate produced by our proposed sparse-recovery method (BADMM) and replacing the interference covariance matrix with the sample covariance matrix obtained from training data, we effectively create a one-step detector (OSD) that combines the sparse recovery algorithm and LRT. Similar to the previous subsection, we utilize the AMF and GLRT as our LRT-based techniques to construct one-step detectors.

1) OSD-BADMM-AMF: For the OSD-BADMM-AMF method we have

$$\begin{aligned}&\Pi_{\text{OSD-BADMM-AMF},m}\\ &= -\left(\mathbf{y} - \hat{x}_m\mathbf{a}(\theta_m)\right)^\dagger\hat{\mathbf{R}}^{-1}(\mathbf{y} - \hat{x}_m\mathbf{a}(\theta_m)) + \mathbf{y}^\dagger\hat{\mathbf{R}}^{-1}\mathbf{y}\\ &= -\left(\mathbf{a}^\dagger(\theta_m)\mathbf{R}^{-1}\mathbf{a}(\theta_m)\right)\left(\hat{x}_m - \frac{\mathbf{a}^\dagger(\theta_m)\mathbf{R}^{-1}\mathbf{y}}{\mathbf{a}^\dagger(\theta_m)\mathbf{R}^{-1}\mathbf{a}(\theta_m)}\right)^2\\ &\quad + \frac{|\mathbf{a}^\dagger(\theta_m)\mathbf{R}^{-1}\mathbf{y}|^2}{\mathbf{a}^\dagger(\theta_m)\mathbf{R}^{-1}\mathbf{a}(\theta_m)}.\end{aligned} \tag{24}$$

By employing the unconstrained maximum likelihood (ML) estimate of x_m:

$$\hat{x}_{\text{ML},m} = \frac{\mathbf{a}^\dagger(\theta_m)\hat{\mathbf{R}}^{-1}\mathbf{y}}{\mathbf{a}^\dagger(\theta_m)\hat{\mathbf{R}}^{-1}\mathbf{a}(\theta_m)}, \tag{25}$$

we obtain

$$\begin{aligned}&\Pi_{\text{OSD-BADMM-AMF},m}\\ &\quad= \Pi_{\text{AMF},m} - (\mathbf{a}^\dagger(\theta_m)\hat{\mathbf{R}}^{-1}\mathbf{a}(\theta_m))|\hat{x}_m - \hat{x}_{\text{ML},m}|^2\\ &\quad= \Pi_{\text{AMF},m} \cdot \left(1 - \frac{|\hat{x}_m - \hat{x}_{\text{ML},m}|^2}{|\hat{x}_{\text{ML},m}|^2}\right),\end{aligned} \tag{26}$$

where $\Pi_{\text{AMF},m}$ represents the decision statistic derived using the steering vector $\mathbf{a}(\theta_m)$. The distinguishing factor between the decision metrics of OSD-ADMM-AMF and its AMF counterpart lies solely in the multiplier expression denoted by $\left(1 - \frac{|\hat{x}_m - \hat{x}_{\text{ML},m}|^2}{|\hat{x}_{\text{ML},m}|^2}\right)$. In scenarios characterized by well-aligned or slightly mismatched signals, and with a high signal-to-interference-plus-noise ratio (SINR), both $\hat{x}_m$ and $\hat{x}_{\text{ML},m}$ typically represent the true amplitude of the signal returned from the target. Consequently, OSD-ADMM-AMF exhibits a behavior similar to AMF under these conditions. However, when dealing with highly mismatched signals, $\hat{x}_m$ equals zero, causing $\Pi_{\text{OSD-ADMM-AMF},m}$ to reflect this descent. This behavior contrasts with $\Pi_{\text{AMF},m}$, which may still exhibit large values in such situations. This insightful observation underscores the significant potential of OSD-ADMM-AMF to outperform AMF in effectively discerning and eliminating undesired signals.

2) OSD-BADMM-GLRT: Based on Kelly's GLRT method, we can achieve the succinct form of

$$\begin{aligned}\max_{\mathbf{R}} \Pi_{\text{LRT},m} &= \left(\frac{\det(\mathbf{T}_0)}{\det(\mathbf{T}_1)}\right)^{K+1}\\ &= \left(\frac{K + \mathbf{y}^\dagger\hat{\mathbf{R}}^{-1}\mathbf{y}}{K + \left(\mathbf{y} - x_m\mathbf{a}(\theta_m)\right)^\dagger\hat{\mathbf{R}}^{-1}\left(\mathbf{y} - x_m\mathbf{a}(\theta_m)\right)}\right)^{K+1}.\end{aligned} \tag{27}$$

By substituting the sparse estimate $\hat{x}_m$ of x_m and employing the first line of equation (24), we formulate the following decision rule:

$$\left(\frac{K + \mathbf{y}^\dagger\hat{\mathbf{R}}^{-1}\mathbf{y}}{K + \mathbf{y}^\dagger\hat{\mathbf{R}}^{-1}\mathbf{y} - \Pi_{\text{OSD-BADMM-AMF},m}}\right) \underset{\text{H}_0}{\overset{\text{H}_1}{\gtrless}} \kappa. \tag{28}$$

Then, by subtracting the denominator from the numerator on both sides of the inequality, and subsequently adding the numerator of the new fraction to its corresponding denominator,

Algorithm 1 TSD-BADMM & OSD-BADMM

Require: κ_{AMF}, κ_{GLRT}, $\kappa_{\text{OSD-BADMM-AMF}}$, $\kappa_{\text{OSD-BADMM-GLRT}}$.
Ensure: H_j: the presence of j targets, with $j = 0, 1$
1: Compute $\hat{\mathbf{x}}$ with BADMM.
2: TSD-BADMM-AMF:
$$\begin{cases} H_0 : |\hat{x}_m| = 0 \text{ or } \Pi_{\text{AMF},m} < \kappa_{\text{AMF}} \\ H_1 : |\hat{x}_m| > 0 \text{ and } \Pi_{\text{AMF},m} > \kappa_{\text{AMF}} \end{cases}$$
3: TSD-BADMM-GLRT:
$$\begin{cases} H_0 : |\hat{x}_m| = 0 \text{ or } \Pi_{\text{GLRT},m} < \kappa_{\text{GLRT}} \\ H_1 : |\hat{x}_m| > 0 \text{ and } \Pi_{\text{GLRT},m} > \kappa_{\text{GLRT}} \end{cases}$$
4: Compute $\Pi_{\text{OSD-BADMM-AMF},m}$ by employing $\hat{x}_{\text{ML}}$ and $\hat{x}$ as indicated in Equation (26).
5: OSD-BADMM-AMF:
$$\Pi_{\text{OSD-BADMM-AMF},m} \underset{\text{H}_0}{\overset{\text{H}_1}{\gtrless}} \kappa_{\text{OSD-BADMM-AMF}}$$
6: Compute $\Pi_{\text{OSD-BADMM-GLRT},m}$ by employing $\hat{x}_{\text{ML}}$ and $\hat{x}$ as indicated in Equation (30).
7: OSD-BADMM-GLRT:
$$\Pi_{\text{OSD-BADMM-GLRT},m} \underset{\text{H}_0}{\overset{\text{H}_1}{\gtrless}} \kappa_{\text{OSD-BADMM-GLRT}}$$

the resulting expression on the left side simplifies to

$$\Pi_{\text{OSD-BADMM-GLRT},m} = \frac{\Pi_{\text{OSD-BADMM-AMF},m}}{K + \mathbf{y}^\dagger \hat{\mathbf{R}}^{-1} \mathbf{y}}. \tag{29}$$

Designating $\hat{x}_{\text{ML},m}$ as the unconstrained maximum likelihood (ML) estimate for x_m, the OSD-BADMM-GLRT statistic takes the form:

$$\Pi_{\text{OSD-BADMM-GLRT},m} = \Pi_{\text{GLRT},m} \cdot \left(1 - \frac{|\hat{x}_m - \hat{x}_{\text{ML},m}|^2}{|\hat{x}_{\text{ML},m}|^2}\right), \tag{30}$$

where $\Pi_{\text{GLRT},m}$, defining the statistical measure of Kelly's GLRT, is expressed as:

$$\Pi_{\text{GLRT},m} = \frac{\Pi_{\text{AMF},m}}{K + \mathbf{y}^\dagger \hat{\mathbf{R}}^{-1} \mathbf{y}}. \tag{31}$$

Algorithm 2 summarizes the suggested decision-making structures in the form of a pseudo-code.

VI. Numerical Case Studies

In this section, we evaluate the performance of the proposed methods—TSD-BADMM-AMF, TSD-BADMM-GLRT, OSD-BADMM-AMF, and OSD-BADMM-GLRT—and compare them with established decision paradigms. Because of the unavailability of a closed-form expression for the false alarm (P_{fa}) and detection (P_d) probabilities, we resort to the use of conventional Monte Carlo techniques for evaluating the methods. For this purpose, we set $P_{\text{fa}} = 10^{-3}$, which implies that the number of Monte Carlo iterations shall be $\frac{100}{P_{\text{fa}}} = 10^5$. We model the interference using an exponentially correlated complex Gaussian vector, wherein a single correlation coefficient denoted by ρ dictates its dynamics. Precisely, the $(i,j)^{th}$ element of the covariance matrix $\mathbf{R}$ conforms to the expression $\rho^{|i-j|}$, where $i, j = 1, \ldots, N$, and the chosen value for ρ stands at 0.95.

We conduct a comprehensive analysis of the P_d characteristics for the proposed methods, covering both matched and mismatched signal scenarios. The nominal pointing direction is set at $0°$. For comparison, we include well-known methods such as the AMF [18], Kelly's GLRT [19], and the Rao detector (RAO)[1] [20]. Additionally, we compare our proposed detectors with the BSLIM-based detectors introduced in [7], which, due to their tunable nature, provide further insight into the analysis. It is noteworthy that the SINR is defined as

$$\text{SINR} = |x|^2 \, \mathbf{a}^\dagger(\theta_t) \, \mathbf{R}^{-1} \, \mathbf{a}(\theta_t). \tag{33}$$

The tests conducted in this study were performed on a machine featuring an Intel Core i7 processor operating at 3.5 GHz with 16 GB of RAM. The system was equipped with an NVIDIA GeForce GTX 3080 graphics card and ran on the Windows 10 operating system. MATLAB R2022a served as the principal tool for data processing and analysis, employing core MATLAB functions and libraries to implement the algorithms.

A. Mismatched Situation

First, our main objective is to evaluate the likelihood of detecting the target in a scenario characterized by mismatched conditions. To simplify this complex scenario, let us consider the case where the nominal angle of arrival (θ_p) is consistently set at $0°$. Thus, when the target's angle of arrival (θ_t) aligns with θ_p, we expect the detector to achieve the maximum detection probability. Conversely, as θ_t deviates from θ_p, we anticipate a decrease in the detection probability. Ideally, the perfect detector showcases maximum selectivity, reaching its lowest probability value when θ_p does not equal θ_t, making it optimal for our analytical objectives. In this part, our goal is to assess the effectiveness of our method compared to both conventional and innovative probability approaches, as we vary parameters like the number of secondary data samples and SINR. This evaluation involves observing the detection probability (P_d) in relation to changes in θ_t.

It is crucial to highlight that methods incorporating the two-step detection (characterized by logical multiplication), consistently yield P_d values either equal to or smaller than their classical counterparts. Consequently, we anticipate TSD-BADMM-AMF to demonstrate P_d values equal to or smaller than the conventional AMF. This also extends to the GLRT, where TSD-BADMM-GLRT is expected to exhibit P_d values equal to or smaller than GLRT. In essence, while two-step detection methods might mimic the classical counterparts in determining precise target locations, their distinctive advantage lies in the improved selectivity.

Focusing on the impact of SINR and the number of secondary data samples, Figures 1 and 2 reveal interesting

[1]For completeness, the RAO formulation is provided as:

$$\Pi_{\text{RAO}} = \frac{|\mathbf{a}^\dagger(\theta) \hat{\mathbf{S}}^{-1} \mathbf{y}|^2}{\mathbf{a}^\dagger(\theta) \hat{\mathbf{S}}^{-1} \mathbf{a}(\theta)}, \tag{32}$$

where $\hat{\mathbf{S}} = \mathbf{y}\mathbf{y}^\dagger + K\hat{\mathbf{R}}$.

patterns. Figure 1 depicts the probability of detection as the antenna beam changes for varying numbers of secondary data samples (11, 14, 18) at $\text{SINR} = 14\,\text{dB}$. We observe a parallel scenario in Figure 2 for $\text{SINR} = 18\,\text{dB}$.

A closer look at conventional statistical approaches, such as AMF and GLRT, reveals that while they achieve high detection probabilities at $\theta_t = 0$ under certain secondary data conditions, they lack selectivity. These methods tend to produce false detections for other targets in the range $(0°, 0.5°)$, which is problematic since the actual target is at $\theta_t = 0°$. As previously emphasized, an ideal detector should maximize detection probability at the true target location while significantly reducing it as the beam deviates, ensuring accuracy and minimizing false detections. Another conventional method, RAO, also exhibits unreliability. Varying SINR and the number of secondary data, it becomes evident that RAO is not an effective detector in mismatched situations. In contrast, methods combining compressive sensing and conventional probability techniques, specifically the fusion of BADMM with AMF and GLRT as a one-step detector (OSD), demonstrate superior performance compared to similar combinations involving BSLIM [7] and other conventional probability methods. Overall, the combination of BADMM with AMF and GLRT outperforms BSLIM in terms of selectivity and probability of target presence. Subsequently, we observe that BSLIM achieves the second-highest rank in terms of both selectivity and detection probability. Furthermore, all combination methods of BADMM and BSLIM as two-step detectors (TSD) exhibit superior selectivity compared to conventional probability algorithms, even approaching the practical similarity to OSD-BADMM methods in Figures 3(b) and 3(c).

In conclusion, one-step detectors utilizing BADMM and BSLIM demonstrate greater robustness and reliability compared to alternative methods. While two-step detectors may not excel in precisely pinpointing the target when θ_t equals θ_p, their strength lies in improved performance in detecting the target's non-existence when $\theta_t \neq \theta_p$.

B. Time Execution

To check the computational complexity of our methods, we provide the average runtime over 10^5 iterations of Monte Carlo simulation. The results reported in Table I clearly demonstrate that the combination of BADMM with conventional methods, particularly using OSD and TSD approaches, surpasses other algorithms in both time execution and complexity. This efficiency stems from the inherent sparsity of the radar scene, which is effectively obtained by the ADMM-based LASSO optimization and BIC after that. By focusing on a sparse vector $\mathbf{x}$, where most entries are zero, the computational burden is significantly reduced. This sparsity minimizes the complexity of combining the results with AMF and GLRT, as many computations involving zero entries can be avoided. In contrast, traditional methods such as RAO, AMF, and GLRT operate on a non-sparse (dense) vector $\mathbf{x}$, which requires more extensive computations.

It is worth to mention that although BSLIM-based algorithms demonstrated better performance in selective target detection compared to RAO, GLRT, and AMF in previous experiments, they fall significantly behind in terms of execution time. While BSLIM-based algorithms [66, 67] also utilize sparsity, they depend on ℓ_q-norm optimization ($0 < q < 1$), which is inherently slower and far more computationally demanding than ADMM. This is because their algorithm must search for the optimum q, a process that adds considerable computational overhead. In contrast, ADMM, one of the fastest algorithms for sparse recovery, efficiently solves the ℓ_1-norm problem using closed-form solutions and achieves rapid convergence.

TABLE I: Analyzing execution time (measured in microseconds) with varying numbers of secondary data.

Algorithm	K=18	K=25	K=32
RAO	1792.556	1496.038	1510.045
AMF	765.732	803.983	803.985
GLRT	1496.038	1510.045	1624.256
OSD-BADMM-AMF	413.070	413.070	413.070
TSD-BADMM-AMF	413.070	413.070	413.070
OSD-BADMM-GLRT	413.444	413.070	395.805
TSD-BADMM-GLRT	530.025	530.034	530.016
OSD-BSLIM-AMF	834.981	834.980	834.981
TSD-BSLIM-AMF	10545.165	10223.749	10156.448
OSD-BSLIM-GLRT	11087.695	10156.336	10237.138
TSD-BSLIM-GLRT	10217.016	11276.528	10217.399

This comparative analysis underscores the effectiveness of BADMM methods in achieving computational efficiency. This solidifies BADMM as a compelling option for scenarios that demand quick and reliable computation.

C. Matched Situation

In this section, we investigate our proposed methodologies under controlled conditions. Assuming the target is located at $\theta_t = 0°$ and the antenna remains stationary, our goal is to assess detection capabilities across varying SINR levels and numbers of secondary data samples. Figure 3 provides a detailed analysis of the performance of traditional techniques, the tunable approach proposed in [7], and our BADMM-based OSD and TSD approaches.

The results clearly indicate that OSD-BADMM-AMF and TSD-BADMM-AMF, even in a matched scenario, can be considered among the most effective detection algorithms. Additionally, for a low number of secondary data samples, the superior performance of OSD-BADMM-AMF becomes evident as the SINR increases, surpassing other algorithms. As the number of secondary data samples increases, nearly all methods strive to become reliable detectors. In summary, the fusion of BADMM with statistical algorithms not only does help in handling a mismatched situation but also proves effective in a matched scenario.

VII. CONCLUSION

In this paper, we introduce two adaptive radar detection structures designed to enhance selectivity and robust detection in the presence of Gaussian interference. These structures utilize LASSO optimization for sparse reconstruction, which is solved using ADMM, integrated with statistical methods

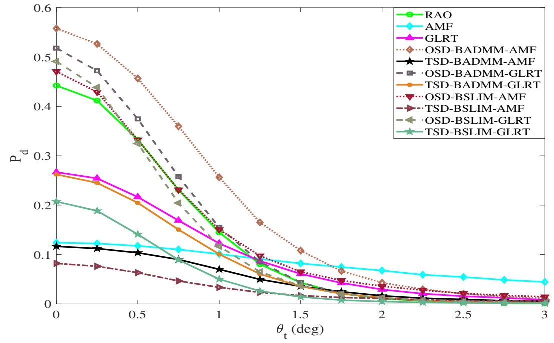

(a)

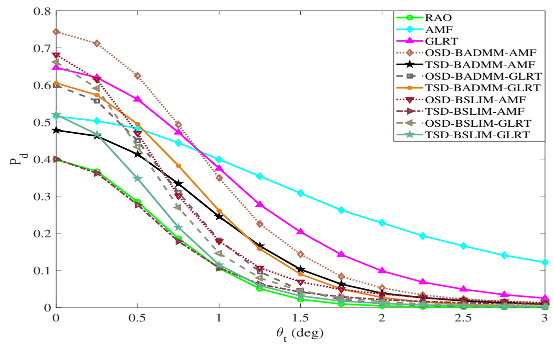

(b)

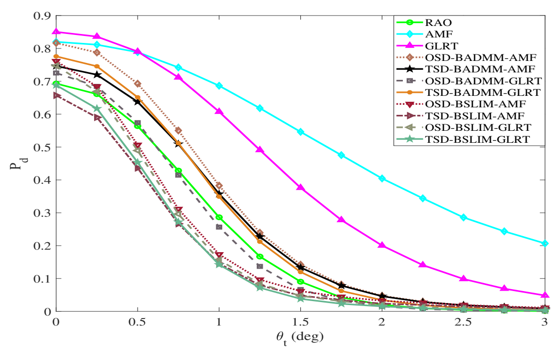

(c)

Fig. 1: Evaluating P_d performance as θ_t varies in the mismatched scenarios at SINR=14 dB for secondary data counts: (a) 11, (b) 14, and (c) 18.

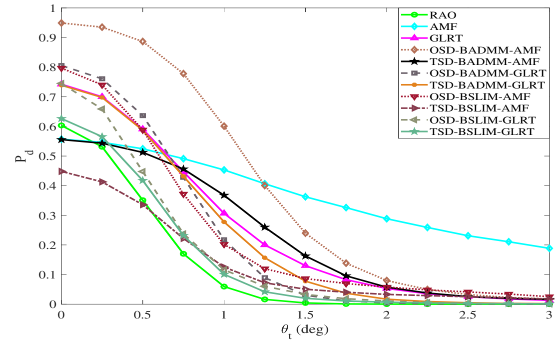

(a)

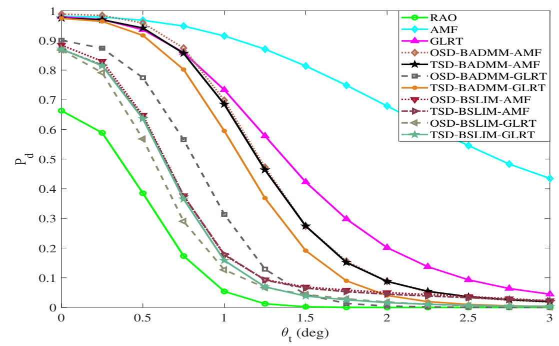

(b)

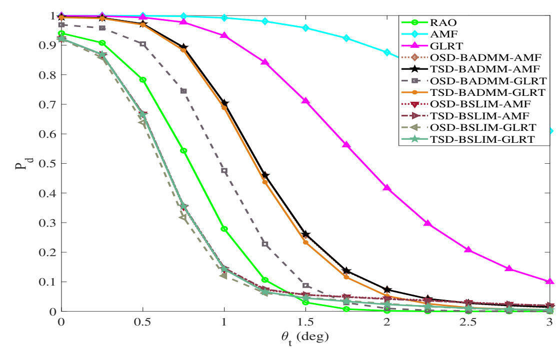

(c)

Fig. 2: Evaluating P_d performance as θ_t varies in the mismatched scenario at SINR=18 dB for secondary data counts: (a) 11, (b) 14, and (c) 18.

such as AMF and GLRT in a joint framework. The proposed approaches outperform traditional statistical algorithms and their main tunable competitors in mismatched scenarios, focusing on selectivity and maximizing detection probability, while also maintaining effective detection in matched scenarios. Additionally, in terms of execution time and complexity, these approaches demonstrate superior performance compared to other competitors.

Future research could focus on extending our proposed techniques to address more challenging radar scenarios, such as those involving non-Gaussian interference or heterogeneous clutter. Furthermore, integrating deep learning approaches, such as recurrent neural networks (RNNs), into sparse recovery frameworks—for example, by utilizing RNNs to update the variables of ADMM—holds significant potential for enhancing detection performance, adaptability, and robustness in dynamic and complex environments.

REFERENCES

[1] J. Liu, K. Li, X. Zhang, M. Liu, and W. Liu, "A weighted detector for mismatched subspace signals," *Signal Processing*, vol. 140, pp. 110–115, 2017.

[2] F. Bandiera, O. Besson, and G. Ricci, "An ABORT-like detector with improved mismatched signals rejection capabilities," *IEEE Transactions on Signal Processing*, vol. 56, no. 1, pp. 14–25, Jan 2008.

[3] C. Hao, B. Liu, S. Yan, and L. Cai, "Parametric adaptive radar detector with enhanced mismatched signals rejection capabilities," *EURASIP Journal on Advances in Signal Processing*, vol. 2010, no. 1, p. 375136, Nov 2010.

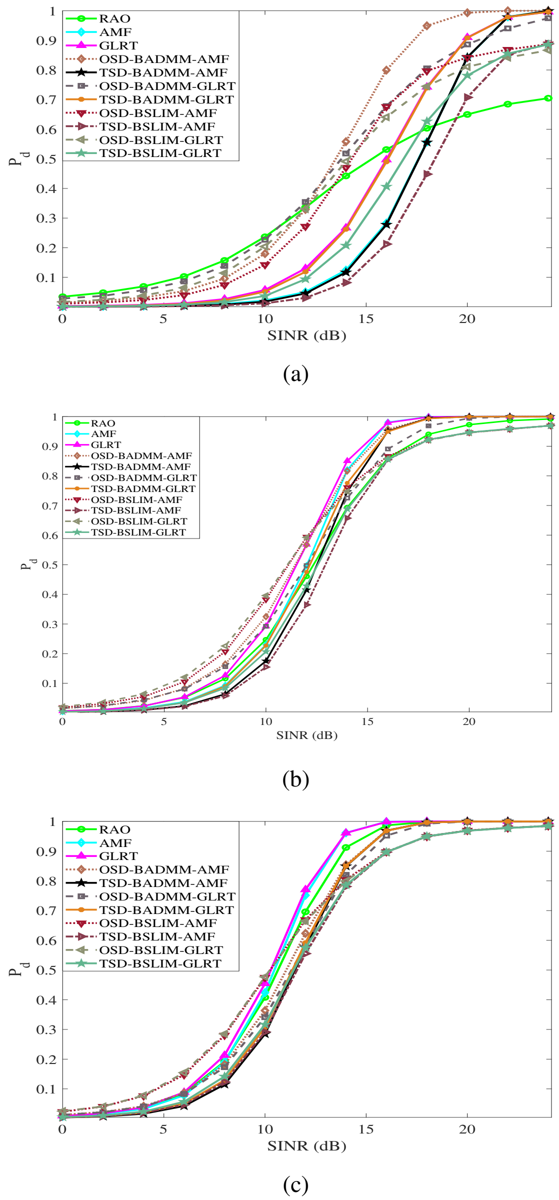

Fig. 3: Evaluating P_d performance as SINR varies in the matched scenario for secondary data counts: (a) 11, (b) 18, and (c) 25.

[4] N. B. Pulsone and C. M. Rader, "Adaptive beamformer orthogonal rejection test," *IEEE Transactions on Signal Processing*, vol. 49, no. 3, pp. 521–529, March 2001.

[5] W. Liu, W. Xie, and Y. Wang, "Parametric detector in the situation of mismatched signals," *IET Radar, Sonar & Navigation*, vol. 8, no. 1, pp. 48–53, January 2014.

[6] A. D. Maio, C. Hao, and D. Orlando, "Two-stage detectors for point-like targets in gaussian interference with unknown spectral properties," in *Modern radar detection theory*. SciTech Publishing Inc, 2016, ch. 4.

[7] S. Han, L. Pallotta, X. Huang, G. Giunta, and D. Orlando, "A sparse learning approach to the design of radar tunable architectures with enhanced selectivity properties," *IEEE Transactions on Aerospace and Electronic Systems*, vol. 56, no. 5, pp. 3840–3853, 2020.

[8] A. Farina and F. Gini, "Interference blanking probabilities for SLB in correlated gaussian clutter plus noise," *IEEE Transactions on Signal Processing*, vol. 48, no. 5, pp. 1481–1485, 2000.

[9] S. Kraut and L. Scharf, "The CFAR adaptive subspace detector is a scale-invariant GLRT," *IEEE Transactions on Signal Processing*, vol. 47, no. 9, pp. 2538–2541, 1999.

[10] C. Richmond, "The theoretical performance of a class of space-time adaptive detection and training strategies for airborne radar," in *Conference Record of Thirty-Second Asilomar Conference on Signals, Systems and Computers*, vol. 2, 1998, pp. 1327–1331 vol.2.

[11] A. Sheikhi, M. Nayebi, and M. Aref, "Adaptive detection algorithm for radar signals in autoregressive interference," *IET Radar, Sonar & Navigation*, vol. 145, no. 5, pp. 309–314, October 1998.

[12] F. Bandiera, D. Orlando, and G. Ricci, "One- and two-stage tunable receivers*," *IEEE Transactions on Signal Processing*, vol. 57, no. 8, pp. 3264–3273, 2009.

[13] C. D. Richmond, "Statistical performance analysis of the adaptive sidelobe blanker detection algorithm," in *Conference Record of the Thirty-First Asilomar Conference on Signals, Systems and Computers*, vol. 1, Nov 1997, pp. 872–876.

[14] C. Hao, B. Liu, and L. Cai, "Performance analysis of a two-stage RAO detector," *Signal Processing*, vol. 91, no. 8, pp. 2141–2146, 2011.

[15] F. Bandiera, D. Orlando, and G. Ricci, *Advanced Radar Detection Schemes Under Mismatched Signal Models*, ser. Synthesis Lectures on Signal Processing. Morgan & Claypool Publishers, 2009.

[16] A. D. Maio, D. Orlando, C. Hao, and G. Foglia, "Adaptive detection of point-like targets in spectrally symmetric interference," *IEEE Transactions on Signal Processing*, vol. 64, no. 12, pp. 3207–3220, June 2016.

[17] D. Orlando and G. Ricci, "A RAO test with enhanced selectivity properties in homogeneous scenarios," *IEEE Transactions on Signal Processing*, vol. 58, no. 10, pp. 5385–5390, Oct 2010.

[18] F. Robey, D. Fuhrmann, E. Kelly, and R. Nitzberg, "A CFAR adaptive matched filter detector," *IEEE Transactions on Aerospace and Electronic Systems*, vol. 28, no. 1, pp. 208–216, 1992.

[19] E. Kelly, "An adaptive detection algorithm," *IEEE Transactions on Aerospace and Electronic Systems*, vol. AES-22, no. 2, pp. 115–127, 1986.

[20] A. De Maio, "RAO test for adaptive detection in gaussian interference with unknown covariance matrix," *IEEE Transactions on Signal Processing*, vol. 55, no. 7, pp. 3577–3584, 2007.

[21] J. Liu, W. Liu, B. Chen, H. Liu, H. Li, and C. Hao, "Modified RAO test for multichannel adaptive signal detection," *IEEE Transactions on Signal Processing*, vol. 64, no. 3, pp. 714–725, Feb 2016.

[22] J. Liu, G. Cui, H. Li, and B. Himed, "On the performance of a persymmetric adaptive matched filter," *IEEE Transactions on Aerospace and Electronic Systems*, vol. 51, no. 4, pp. 2605–2614, Oct 2015.

[23] A. D. Maio and D. Orlando, "Feature article: A survey on two-stage decision schemes for point-like targets in gaussian interference," *IEEE Aerospace and Electronic Systems Magazine*, vol. 31, no. 4, pp. 20–29, April 2016.

[24] K. Cui, Y. Gao, Z. Zhang, and L. Zuo, "Persymmetric design of jointly detection and bearing estimation for a 2D array radar in training demanding scenarios," *Digital Signal Processing*, vol. 148, p. 104458, 2024.

[25] D. Manolakis, T. Cooley, and J. Jacobson, "Effects of signature mismatch on hyperspectral detection algorithms," in *2010 2nd Workshop on Hyperspectral Image and Signal Processing: Evolution in Remote Sensing*, 2010, pp. 1–4.

[26] O. Besson, L. L. Scharf, and S. Kraut, "Adaptive detection of a signal known only to lie on a line in a known subspace, when primary and secondary data are partially homogeneous," *IEEE Transactions on Signal Processing*, vol. 54, no. 12, pp. 4698–4705, 2006.

[27] C. Hao, J. Yang, and C. Hou, "Adaptive radar detection of distributed targets with orthogonal rejection," in *2011 IEEE RadarCon (RADAR)*, 2011, pp. 058–061.

[28] C. H. Lim, E. Aboutanios, and B. Mulgrew, "Adaptive array detection algorithms with steering vector mismatch," in *2006 14th European Signal Processing Conference*, 2006, pp. 1–5.

[29] A. Coluccia, D. Orlando, and G. Ricci, "A GLRT-like CFAR detector for heterogeneous environments," *Signal Processing*, vol. 194, p. 108401, 2022.

[30] A. M. Rekavandi, "Towards adaptive subspace detection in heterogeneous environment," *arXiv preprint arXiv:2401.12469*, 2024.

[31] E. Conte and G. Ricci, "Sensitivity study of GLRT detection in compound-Gaussian clutter," *IEEE Transactions on Aerospace and Electronic Systems*, vol. 34, no. 1, pp. 308–316, 1998.

[32] Z. Wang, Z. He, Q. He, B. Xiong, and Z. Cheng, "Adaptive polarimetric detection for mismatched signal in non-gaussian sea clutter," in *2022 IEEE Radar Conference (RadarConf22)*, 2022, pp. 1–6.

[33] F. Bandiera, A. D. Maio, A. S. Greco, and G. Ricci, "Adaptive radar detection of distributed targets in homogeneous and partially homogeneous noise plus subspace interference," *IEEE Transactions on Signal Processing*, vol. 55, no. 4, pp. 1223–1237, April 2007.

[34] F. Bandiera, O. Besson, D. Orlando, G. Ricci, and L. L. Scharf, "GLRT-based direction detectors in homogeneous noise and subspace interference," *IEEE Transactions on Signal Processing*, vol. 55, no. 6, pp. 2386–2394, June 2007.

[35] S. Kraut, L. L. Scharf, and L. T. McWhorter, "Adaptive subspace detectors," *IEEE Transactions on Signal Processing*, vol. 49, no. 1, pp. 1–16, Jan 2001.

[36] L. Mao, Y. Gao, S. Yan, and L. Xu, "Persymmetric subspace detection in structured interference and non-homogeneous disturbance," *IEEE Signal Processing Letters*, vol. 26, no. 6, pp. 928–932, 2019.

[37] J. Liu, T. Jian, and W. Liu, "Persymmetric detection of subspace signals based on multiple observations in the presence of subspace interference," *Signal Processing*, vol. 183, p. 107964, 2021.

[38] S. Kraut and L. L. Scharf, "The CFAR adaptive subspace detector is a scale-invariant GLRT," *IEEE Transactions on Signal Processing*, vol. 47, no. 9, pp. 2538–2541, Sep. 1999.

[39] D. Adamy, *EW101: A first course in electronic warfare*. Norwood, MA: Artech House, 2001.

[40] F. Bandiera, D. Orlando, and G. Ricci, "A subspace-based adaptive sidelobe blanker," *IEEE Transactions on Signal Processing*, vol. 56, no. 9, pp. 4141–4151, 2008.

[41] F. Bandiera, O. Besson, D. Orlando, and G. Ricci, "An improved adaptive sidelobe blanker," *IEEE Transactions on Signal Processing*, vol. 56, no. 9, pp. 4152–4161, 2008.

[42] F. Bandiera, D. Orlando, and G. Ricci, "Adaptive radar detection of distributed targets under conic constraints," in *2008 IEEE Radar Conference*, 2008, pp. 1–6.

[43] ——, "A parametric adaptive radar detector," in *2008 IEEE Radar Conference*, 2008, pp. 1–5.

[44] F. Bandiera, A. De Maio, and G. Ricci, "Adaptive CFAR radar detection with conic rejection," *IEEE Transactions on Signal Processing*, vol. 55, no. 6, pp. 2533–2541, 2007.

[45] M. Greco, F. Gini, and A. Farina, "Radar detection and classification of jamming signals belonging to a cone class," *IEEE Transactions on Signal Processing*, vol. 56, no. 5, pp. 1984–1993, 2008.

[46] Y. I. Abramovich, N. K. Spencer, and A. Y. Gorokhov, "Modified GLRT and AMF framework for adaptive detectors," *IEEE Transactions on Aerospace and Electronic Systems*, vol. 43, no. 3, pp. 1017–1051, 2007.

[47] B. Xiong, Z. Wang, Q. He, and Z. He, "Model-based adaptive detector of range-spread targets with secondary data support," in *IGARSS 2022 - 2022 IEEE International Geoscience and Remote Sensing Symposium*, 2022, pp. 2789–2792.

[48] F. Bandiera, O. Besson, D. Orlando, and G. Ricci, "Theoretical performance analysis of the W-ABORT detector," *IEEE Transactions on Signal Processing*, vol. 56, no. 5, pp. 2117–2121, 2008.

[49] O. Besson and D. Orlando, "Adaptive detection in nonhomogeneous environments using the generalized eigenrelation," *IEEE Signal Processing Letters*, vol. 14, no. 10, pp. 731–734, 2007.

[50] G. Capraro, A. Farina, H. Griffiths, and M. Wicks, "Knowledge-based radar signal and data processing: a tutorial review," *IEEE Signal Processing Magazine*, vol. 23, no. 1, pp. 18–29, 2006.

[51] G. Fabrizio, A. Farina, and M. Turley, "Spatial adaptive subspace detection in oth radar," *IEEE Transactions on Aerospace and Electronic Systems*, vol. 39, no. 4, pp. 1407–1428, 2003.

[52] N. Pulsone and C. Rader, "Adaptive beamformer orthogonal rejection test," *IEEE Transactions on Signal Processing*, vol. 49, no. 3, pp. 521–529, 2001.

[53] F. Bandiera, O. Besson, and G. Ricci, "An ABORT-like detector with improved mismatched signals rejection capabilities," *IEEE Transactions on Signal Processing*, vol. 56, no. 1, pp. 14–25, 2008.

[54] C. Richmond, "Performance of a class of adaptive detection algorithms in nonhomogeneous environments," *IEEE Transactions on Signal Processing*, vol. 48, no. 5, pp. 1248–1262, 2000.

[55] R. J. A. T. K. D. Ward and S. Watts, "Sea clutter: Scattering, the K distribution and radar performance," *Waves in Random and Complex Media*, vol. 17, no. 2, pp. 233–234, 2007.

[56] S. Kraut, L. Scharf, and L. McWhorter, "Adaptive subspace detectors," *IEEE Transactions on Signal Processing*, vol. 49, no. 1, pp. 1–16, 2001.

[57] A. De Maio, "Robust adaptive radar detection in the presence of steering vector mismatches," *IEEE Transactions on Aerospace and Electronic Systems*, vol. 41, no. 4, pp. 1322–1337, 2005.

[58] D. Manolakis and G. Shaw, "Detection algorithms for hyperspectral imaging applications," *IEEE Signal Processing Magazine*, vol. 19, no. 1, pp. 29–43, 2002.

[59] F. Gini, A. Farina, and M. Greco, "Selected list of references on radar signal processing," *IEEE Transactions on Aerospace and Electronic Systems*, vol. 37, no. 1, pp. 329–359, 2001.

[60] Q. Guo, L. Liu, S. Huang, M. Kaliuzhnyi, and V. Tuz, "Adaptive detectors for mismatched subspace target in clutter with lognormal texture," *Digital Signal Processing*, vol. 154, p. 104692, 2024.

[61] E. Kelly, "Performance of an adaptive detection algorithm; rejection of unwanted signals," *IEEE Transactions on Aerospace and Electronic Systems*, vol. 25, no. 2, pp. 122–133, 1989.

[62] R. Tibshirani, "Regression shrinkage and selection via the lasso," *Journal of the Royal Statistical Society Series B: Statistical Methodology*, vol. 58, no. 1, pp. 267–288, 1996.

[63] P. Stoica and Y. Selen, "Model-order selection: a review of information criterion rules," *IEEE Signal Processing Magazine*, vol. 21, no. 4, pp. 36–47, 2004.

[64] S. Boyd, N. Parikh, E. Chu, B. Peleato, J. Eckstein, *et al.*, "Distributed optimization and statistical learning via the alternating direction method of multipliers," *Foundations and Trends® in Machine learning*, vol. 3, no. 1, pp. 1–122, 2011.

[65] Y. Yang, X. Guan, Q.-S. Jia, L. Yu, B. Xu, and C. J. Spanos, "A survey of ADMM variants for distributed optimization: Problems, algorithms and features," *arXiv preprint arXiv:2208.03700*, 2022.

[66] X. Tan, W. Roberts, J. Li, and P. Stoica, "Sparse learning via iterative minimization with application to MIMO radar imaging," *IEEE Transactions on Signal Processing*, vol. 59, no. 3, pp. 1088–1101, 2011.

[67] M. Jabbarian-Jahromi and M. H. Kahaei, "Two-dimensional SLIM with application to pulse doppler MIMO radars," *EURASIP Journal on Advances in Signal Processing*, vol. 2015, pp. 1–12, 2015.